

# Characterizing the solid-state thermal oxidation of poly(ethylene oxide) powder

John Scheirs\*, Stephen W. Bigger† and Oskar Delatycki

Department of Industrial Science, The University of Melbourne, Parkville 3052, Australia

(Received 23 February 1990; revised 29 June 1990; accepted 3 July 1990)

The oxidative degradation of powdered poly(ethylene oxide) (PEO) resin was studied by polarized optical microscopy, scanning electron microscopy (SEM), differential scanning calorimetry (d.s.c.), solution viscometry and Fourier-transform infra-red spectroscopy (FTi.r.). Powdered PEO readily oxidizes under mild ageing conditions (60°C) owing to its large surface area, its strained crystalline lattice and the weak carbon–oxygen bonds in its backbone. As a result, its physical properties deteriorate after an induction period of about 23 days and, in the extreme case, the free-flowing powder is transformed into a soft wax. With increasing oxidation, there is also a pronounced change in the morphology of PEO from a spherulitic to an axialitic structure. This transition is due to oxidatively induced changes in molecular weight and dispersity that affect the crystallization conditions. Examination of the PEO powder by SEM shows that it has an intricate, fibrillar, surface structure, which produces a large surface area available for oxidation. The emergence of multiple d.s.c. melting peaks after oxidation indicates that a number of low-melting, low-molecular-weight fractions are formed as a result of chain scission processes.

(Keywords: poly(ethylene oxide); thermal oxidation; spherulites; axialites; Fourier-transform infra-red spectroscopy; scanning electron microscopy; differential scanning calorimetry)

## INTRODUCTION

Poly(ethylene oxide) (PEO) has a unique combination of properties. It is a tough, ductile, highly crystalline thermoplastic and is readily soluble in water, where it displays interesting hydrodynamic, flocculating<sup>1</sup> and drag-reducing properties<sup>2</sup>. High-molecular-weight PEO ( $M_w > 1.0 \times 10^5$ ) is used for water-soluble packaging film<sup>3</sup>. Films of PEO are flexible, strong, 'breathable', heat-sealable and relatively resistant to atmospheric moisture because of their high degree of crystallinity<sup>3</sup>. Water-soluble PEO films are used for 'disposable' laundry bags<sup>4</sup> as well as packaging for agricultural seeding<sup>5</sup>, hazardous dyes and detergents<sup>4</sup>. Low-molecular-weight PEO is used widely as a chromatographic stationary phase<sup>6</sup> (Carbowax®) and as the major component in wet-tack adhesives<sup>7</sup>.

The spherulitic structure of melt-crystallized PEO has been reported widely<sup>8,9</sup>. Extensive studies have revealed anomalous crystallization kinetics<sup>10</sup> as well as a lack of correlation between the glass transition temperature and spherulitic growth rate<sup>11</sup>. The cause of these inconsistencies has been attributed to degradation resulting from the excessive exposure to high temperatures used in the experiments<sup>10</sup>. The crystallization characteristics of the sample are thereby obscured because they are strongly dependent on the molecular weight and weight distribution. Furthermore, the extensive degradation of PEO during size exclusion chromatography demonstrates its sensitivity to shear<sup>12</sup>.

A number of researchers have found that PEO undergoes marked thermo-oxidative<sup>13</sup> and mechanical<sup>2,14</sup> degradation. The sensitivity of PEO to free-radical oxidative attack during storage and the reduction of

molecular weight under shear are factors that make difficult the characterization of the polymer<sup>2</sup>. Freshly polymerized, unstabilized PEO degrades rapidly in 18 days at ambient temperature<sup>15</sup>. Significant oxidation of PEO occurs when it is stored in bulk at ambient temperature for 2–4 years<sup>13</sup> and measurable degradation occurs in the absence of oxygen and light<sup>15</sup>.

The oxidation of PEO has been studied, using viscometry, in aqueous and organic solutions<sup>16</sup> as well as in the melt<sup>6,17,18</sup>. However, little information concerning the solid-state thermal oxidation of PEO appears in the literature to date. Aqueous solutions of PEO are sensitive to aerobic oxidation at temperatures as low as 40°C and it has been reported<sup>19</sup> that the viscosity of a 0.1% (w/v) aqueous solution of unstabilized PEO is reduced by about 95% after 5 h heating at 100°C. Furthermore, solution viscometry experiments have shown that polymers containing oxygen in the main chain tend to degrade more readily than those containing only carbon atoms in their backbone<sup>20</sup>. This is because the carbon–oxygen bond energy is lower than that of the carbon–carbon bond in these cases<sup>21</sup>.

Poly(ethylene oxide) is particularly suitable for morphological studies using polarized optical microscopy since it shows large, well-defined spherulites and its nucleation and growth rates can be varied and recorded easily<sup>8,22</sup>. The kinetics of melt crystallization are affected by molecular weight and polydispersity as well as the length and concentration of chain branches. In the case of PEO the changes in these properties caused by thermal oxidation can be observed in terms of the dramatic changes that are imposed on the morphology of the spherulites. Thus, polarized optical microscopy can be conveniently used to assess the effect of thermal oxidation.

Typical commercial applications of PEO require that it has adequate thermo-oxidative stability during bulk

\* To whom correspondence should be addressed

† Present address: Faculty of Applied Science, Western Institute, McKechnie Street, St Albans 3021, Australia

0032-3861/91/112014-06

© 1991 Butterworth-Heinemann Ltd.

storage, melt processing and use. Furthermore, in view of the fact that PEO oxidizes rapidly in the solid state under mild thermal conditions, causing a dramatic loss of its physical properties, the effect of thermal oxidation on the spherulitic morphology and molecular parameters was investigated.

## EXPERIMENTAL

### Materials and sample preparation

A standard PEO homopolymer powder with  $\bar{M}_w$  of  $1 \times 10^5 \text{ g mol}^{-1}$  was obtained from Aldrich Chemical Company. The polymer contained no additives and was used as received. The powder was oxidized in glass dishes in a thermostated air-circulating oven at  $60 \pm 0.5^\circ\text{C}$ . The polymer was aged for a total of 33 days and samples were taken daily.

### Viscosity-average molecular weight

Solutions of PEO in benzene for viscometry measurements were prepared by gentle heating. In this solvent, PEO does not thermally degrade over extended periods<sup>16</sup>. Vigorous stirring was avoided because it has been reported that chain cleavage can result from shearing of the solution<sup>3</sup>. A concentration range of 0.25–2.0% (w/v) was used, since at lower concentrations the Huggins plot displays a severe dependence on the accuracy of the flow times, while at higher concentrations the solutions have non-Newtonian flow characteristics<sup>23</sup>.

Viscosities were measured at  $25 \pm 0.1^\circ\text{C}$  using an Ubbelohde-type capillary viscometer. The flow time of the pure solvent was 158 s. The kinetic energy and shear corrections<sup>24</sup> were negligibly small. Intrinsic viscosities were determined using a method described elsewhere<sup>25</sup>. Viscosity-average molecular weights ( $\bar{M}_v$ ) were calculated from the intrinsic viscosity values by the Mark–Houwink equation<sup>26</sup>. The  $\bar{M}_v$  of the unoxidized PEO used in this study was measured as  $1.02 \times 10^5 \text{ g mol}^{-1}$ . Assuming that the PEO has a narrow molecular-weight distribution, the average molecular-weight values quoted by the manufacturer and measured in this work are comparable within experimental error.

### Scanning electron microscopy (SEM)

Samples for SEM examination were mounted on aluminium stubs with double-sided adhesive tape. The samples were coated with a 30 nm layer of gold in a vacuum sputterer in order to prevent charging. Electron micrographs were taken on an Hitachi model S570 scanning electron microscope equipped with a lanthanum hexaboride ( $\text{LaB}_6$ ) crystal electron source. This source has a greater electron efficiency than conventional tungsten sources and was operated at a voltage of 5 kV to reduce electron beam damage of the delicate microstructure of the polymer powder.

### Infra-red analysis

Samples of PEO were cast onto NaCl plates from 1.0% (w/v) chloroform solution and examined with a Mattson FTi.r. using the transmission mode. Infra-red spectra were obtained by averaging 16 scans of each sample.

### Differential scanning calorimetry (d.s.c.)

Melting endotherms and crystallinities were determined using a Perkin–Elmer DSC-7 calorimeter with a

standard heating and cooling rate of  $10^\circ\text{C min}^{-1}$ . Samples of approximately 10 mg were run in a nitrogen atmosphere over the temperature range 25 to  $80^\circ\text{C}$ . Indium ( $T_m=156.6^\circ\text{C}$ ) and azobenzene ( $T_m=68.5^\circ\text{C}$ ) were used for temperature calibration. The degree of crystallinity was calculated from the ratio of the experimentally determined enthalpy of melting of a sample,  $\Delta H_m$ , to that of 100% crystalline PEO<sup>27,28</sup>.

### Polarized optical microscopy

An Olympus model OM-2 optical microscope was used to obtain the polarized optical micrographs. The polymer samples were pressed between a coverslip and slide on a Mettler FP82 hot stage. The films were first melted at  $85^\circ\text{C}$  for 3 min to obtain a relaxed melt and to destroy all crystal nuclei<sup>29</sup>, then cooled rapidly and crystallized isothermally at  $61^\circ\text{C}$ . It was necessary to press the PEO into very thin films ( $\sim 15 \mu\text{m}$ ), since in thicker films the nucleation and growth rates are functions of film thickness<sup>22</sup>.

## RESULTS AND DISCUSSION

### Viscosity-average molecular weight

The thermal oxidation of PEO at  $60^\circ\text{C}$  causes a considerable change in its physical properties. Figure 1 shows the change in  $\bar{M}_v$  of PEO with oven ageing at  $60^\circ\text{C}$  in air. The molecular weight decreases slowly during the initial 23 days. This is followed by a severe drop in molecular weight during the auto-accelerating stage of the free-radical degradative process.

After 30 days of thermal oxidation, PEO is transformed from a free-flowing powder to a soft, waxy solid. The susceptibility of PEO to degradation at relatively low temperatures has been reported previously<sup>15</sup>. Poly(ethylene oxide) has a much lower resistance to thermal degradation than polyethylene<sup>30</sup> and this may be attributable to dipole–dipole interactions between neighbouring methylene and oxygen groups<sup>15</sup>. These lead to exceptionally high strains in the helical crystalline

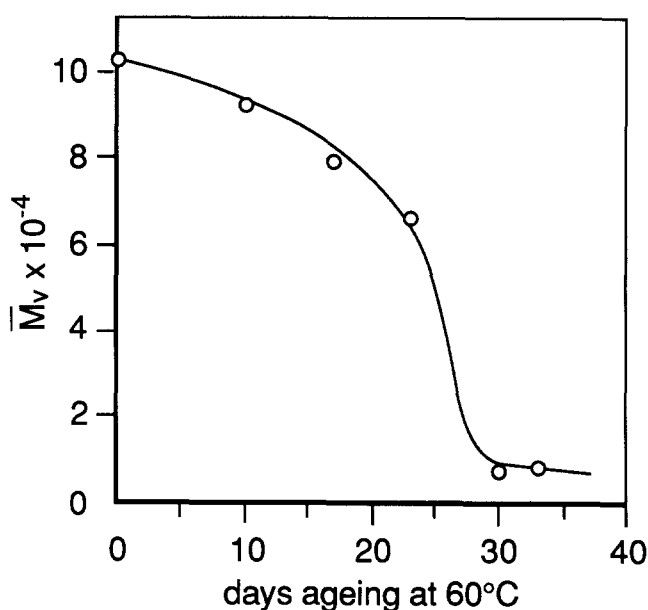


Figure 1 Viscosity-average molecular weight ( $\bar{M}_v$ ) of PEO as a function of ageing time (days) at  $60^\circ\text{C}$

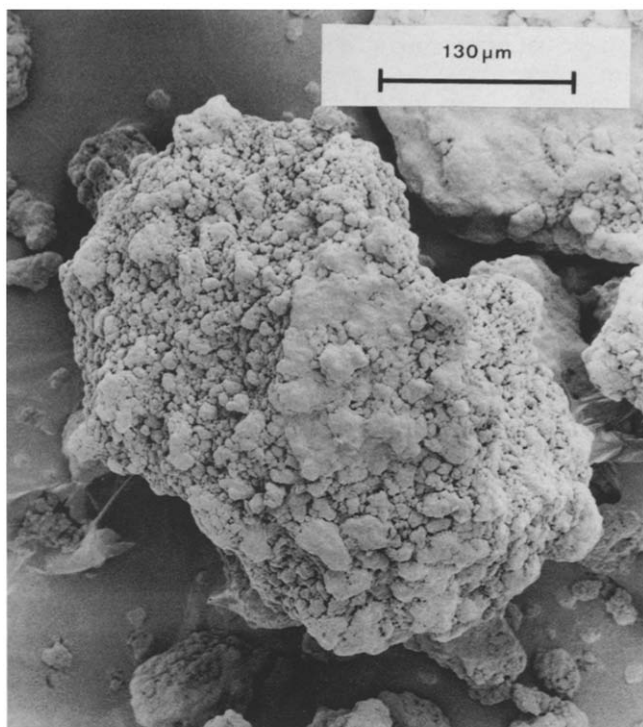


Figure 2 Micrograph of a granule of unoxidized PEO

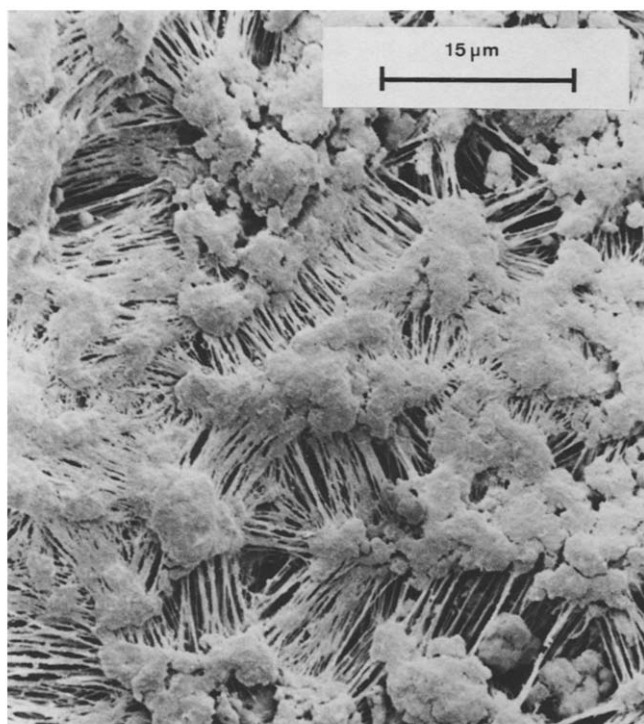


Figure 3 Micrograph of the surface of a granule of unoxidized PEO

structure. In particular, the energy associated with the tension in a chain composed of 11 oxyethylene units is comparable to the covalent bond energy of a carbon-oxygen bond<sup>15</sup>. In addition, the high strains present at the chain folds of the lamellae lower the activation energy of hydrogen abstraction, so that these regions are more susceptible to free-radical attack<sup>31</sup>.

#### Scanning electron micrographs

Examination of the PEO powder by electron micro-

scopy shows that it consists of particles less than 200  $\mu\text{m}$  in diameter which possess a rough surface texture (see Figure 2). Figure 3 is a micrograph of the surface of a granule of PEO at high magnification. The surface consists of an intricate array of cobweb-like structures similar to those observed previously in nascent high-density polyethylene (HDPE)<sup>32,33</sup>. The small granular size of the PEO powder combined with the fibrillar surface morphology leads to high rates of oxidation. Thus, it is likely that the susceptibility of PEO to oxidation is influenced by the unhindered diffusion of oxygen as well as crystalline strain effects.

Figure 4 shows the surface of a granule of PEO after 23 days of thermal oxidation at 60°C. Considerable changes to the structure that have occurred include a substantial reduction in the size of the agglomerates as well as a shortening and thickening of the interconnecting fibrils. These changes may be ascribed to the partial melting and flow of low-molecular-weight fractions that are produced by oxidation. The remaining fibrils are probably more resistant to melting owing to their strain-induced orientation.

#### Infra-red analysis

Figure 5 shows the Fourier-transform infra-red (FTIR) spectrum of PEO after 0, 23 and 33 days of thermal oxidation at 60°C. The broad peak centred at  $\sim 1720\text{ cm}^{-1}$  comprises overlapping, unresolved, aldehyde, ester and dimerized carboxylic acid absorptions. The aldehyde species appears to be the most abundant product of thermal oxidation<sup>30,34</sup>. The shoulder near  $1747\text{ cm}^{-1}$  is an ester absorption<sup>35</sup>. It is interesting to note that, in the early stages of oxidation, the ester and the combined carbonyl/carboxylic acid absorptions are of similar magnitude. However, as the oxidation proceeds further, the carbonyl/carboxylic acid absorption exceeds that of

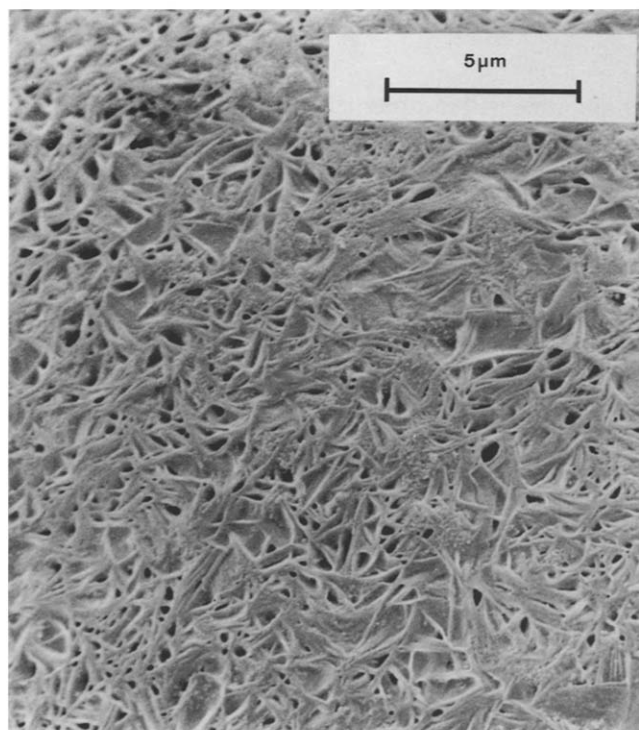


Figure 4 Micrograph of the surface of a granule of PEO oxidized for 23 days

transmission (%)

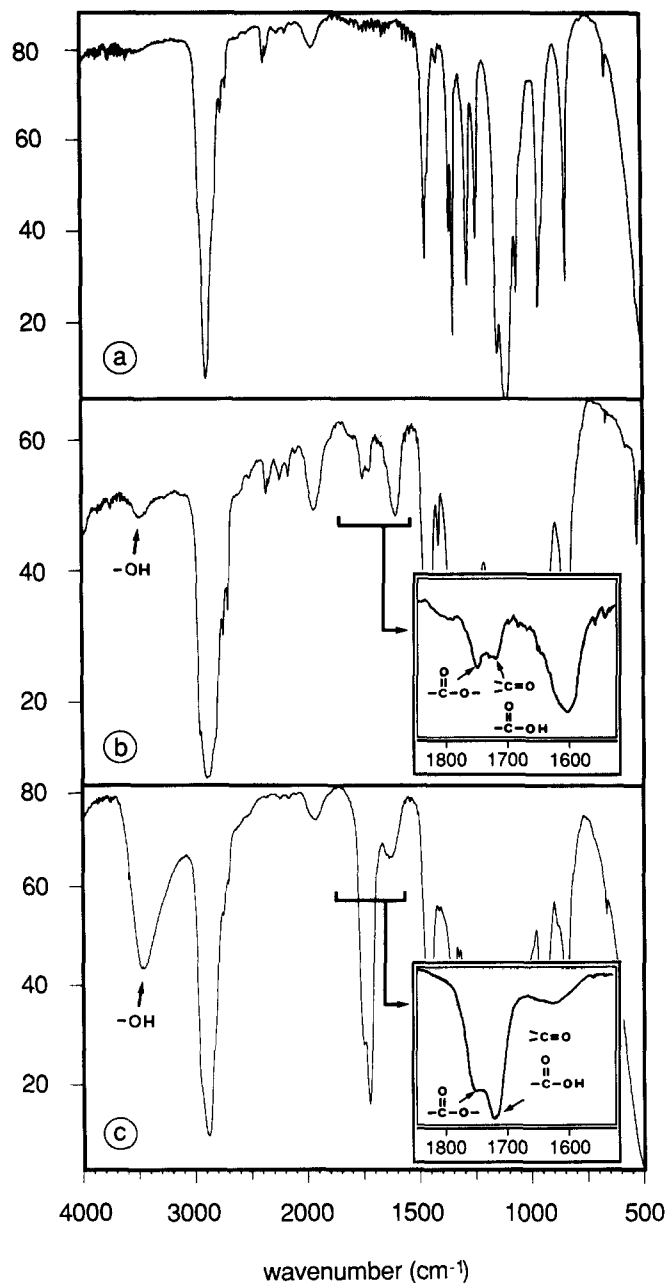


Figure 5 Fourier-transform infra-red spectra of PEO aged for (a) 0 days, (b) 23 days and (c) 33 days

the ester (see Figure 5c). The hydroxyl absorption at approximately  $3500\text{ cm}^{-1}$  increases rapidly after an induction period of about 23 days and masks the hydroperoxide absorption owing to the larger extinction coefficient of the hydroxyl group. The band centred at  $1600\text{ cm}^{-1}$  arises from cyclic, conjugated oxidation products and increases in intensity until the onset of autocatalytic degradation, after which it remains constant.

The FTi.r. spectra provide evidence to support the notion of a free-radical, chain mechanism of oxidative degradation<sup>36</sup> in which hydroperoxide groups accumulate during the induction period until a critical concentration is reached. These subsequently decompose to form oxygenated groups along with concomitant chain scission. It should be noted, however, that oxygenated function-

alities, such as carbonyl groups, can also be produced by the anaerobic thermal degradation of polyethers<sup>21</sup>.

#### Differential scanning calorimetry (d.s.c.)

Figure 6a shows that PEO aged for 23 days has a marginally higher crystallinity (85%) than the unoxidized polymer (84%). Other researchers have reported that the crystallinity of PEO increases with oxidative degradation<sup>15</sup>. This may be attributable to hydrogen bonding of the hydroxyl and carboxylic acid groups to the ether bonds in the backbone<sup>11,37</sup>. Similarly, an increase in crystallinity as a result of oxidative degradation has been observed for polyethylene<sup>38</sup>. The development of a small peak in the trace of the sample aged for 23 days is due to the incipient formation of low-molecular-weight oxidation products.

The sample aged for 33 days (see Figure 6b) has a crystallinity of 42%. The d.s.c. data show that thermal oxidation produces two distinct melting peaks (62 and  $52^\circ\text{C}$ ). This confirms that chain scission produces lower-molecular-weight material with two discrete ranges of lamellar thickness. The existence of multiple melting peaks has been related to the varying number of chain folds in the crystals<sup>39,40</sup>. The peak melting temperature (see Figure 6b) is depressed approximately  $7^\circ\text{C}$  compared with that of the unoxidized polymer owing to the presence of the low-molecular-weight component. These results are consistent with those obtained by Cheng and

heat flow (mW)

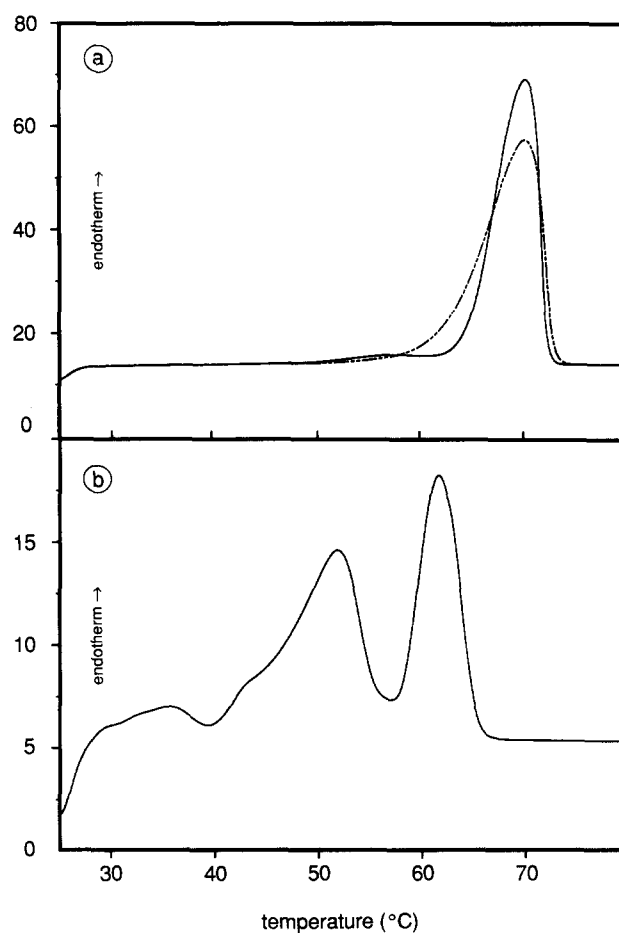
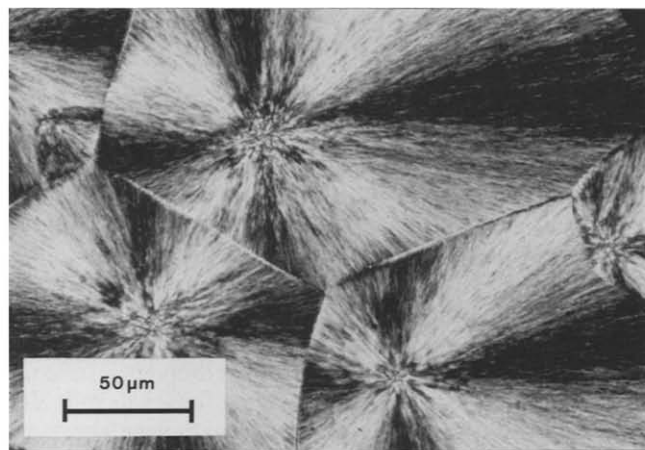
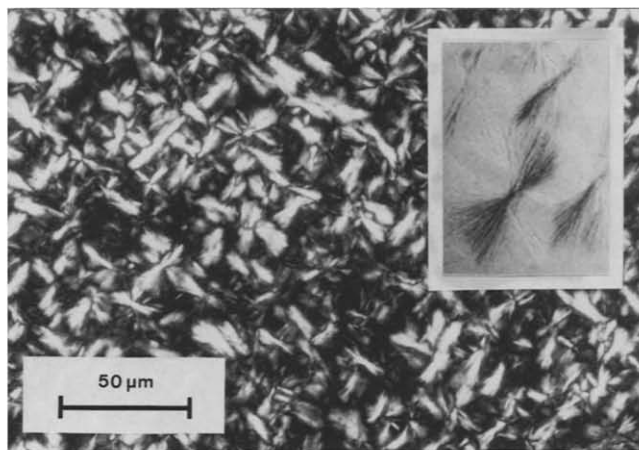


Figure 6 D.s.c. traces of PEO aged for (a) 0 days (chain curve) and 23 days (full curve) and (b) 33 days



**Figure 7** Polarized optical micrograph of unoxidized PEO isothermally crystallized at 61°C



**Figure 8** Polarized optical micrograph of PEO oxidized for 33 days and isothermally crystallized at 61°C. Inset: axialites shown at 2.5 times higher magnification

Wunderlich<sup>41</sup> using an isothermally crystallized sample of pure PEO ( $\bar{M}_w = 1.0 \times 10^5$ ) containing approximately 28% (w/w) of a low-molecular-weight ( $\bar{M}_w = 3.5 \times 10^3$ ) component. This blend shows melting peaks at 62 and 57°C.

#### Polarized optical micrographs

Figure 7 shows PEO spherulites in an unoxidized sample. The spherulites are negatively birefringent with a coarsely fibrous, radiating texture and have the characteristic 'Maltese cross' pattern, which indicates spherical symmetry. The spherulites are extremely large (approximately 200 μm in diameter) and are similar in size to those reported elsewhere<sup>9,42</sup>. Figure 8 shows the supermolecular structure of oxidized PEO, which contains needle-like axialites that are surrounded by a non-birefringent, amorphous region. The axialites are precursors in the rudimentary stage of spherulitic growth and their full development has been curtailed by the high concentration of non-crystallizable degradation products. In the morphological map of PEO constructed by Allen and Mandelkern<sup>9</sup>, axialites ('hedrites') predominantly occur in the region corresponding to low molecular weight and high crystallization temperatures. This is consistent with the findings of the present study, where the axialites grow within a melt containing significant amounts of oligomeric oxidation products. Furthermore, it has been shown that low-molecular-weight oxidation products formed in PEO cause it to behave similarly to PEO systems that are loaded with large amounts of low-molecular-weight species<sup>43,44</sup>. The solid-state, thermal oxidation of HDPE also produces an axialitic morphology when the polymer is crystallized isothermally from the melt<sup>45</sup>. The morphological similarity between HDPE and PEO has been reported previously<sup>9,46</sup>.

#### CONCLUSIONS

Poly(ethylene oxide) is oxidized easily at moderate temperatures and this causes a rapid decrease in solution viscosity, the appearance of multiple, lower-temperature melting peaks in the d.s.c. trace as well as the formation of appreciable quantities of aldehyde, carboxylic acid and hydroxyl groups. The multiple melting peaks are due to the segregation of low-molecular-weight oxidation pro-

ducts and may be associated with the number of chain folds in the lamellae. Scanning electron micrographs of the surface of PEO show a complex network of drawn fibrils, which produce a large surface-to-volume ratio. This is an important contributing factor to the rapid rate of thermal oxidation of the polymer at low temperatures. Poly(ethylene oxide) powder aged at 60°C has an induction period of 23 days, which is followed by rapid oxidation by a free-radical chain mechanism. The morphology of isothermally crystallized PEO is altered significantly as a result of oxidation and it changes from large spherulites with a radiating fibrous texture to sharp needle-like axialites. There is a slight increase in percentage crystallinity after 23 days of oxidation. However, after 33 days of thermal oxidation, the crystallinity is reduced by approximately one-half.

#### ACKNOWLEDGEMENTS

The authors are grateful to Commercial Polymers Australia Ltd and The University of Melbourne, Special Initiatives Grants Scheme, for financial support; the Department of Material Engineering, Monash University, for the use of its polarizing optical microscopy facility; Dr W. D. Cook of the Dental Products and Medical Devices Laboratory for assistance with the d.s.c. measurements; Dr G. Heath of the CSIRO Division of Chemicals and Polymers for help with the FTi.r. spectra; and Mr G. J. Pratt of the Department of Industrial Science, The University of Melbourne, for reading the manuscript.

#### REFERENCES

- 1 Powell, G. M. and Bailey, F. E. in 'Kirk-Othmer Encyclopedia of Chemical Technology', Wiley-Interscience, New York, 1960, 2nd Suppl. Vol., pp. 597-609
- 2 Fisher, D. H. and Rodriguez, F. J. *Appl. Polym. Sci.* 1971, **15**, 2975
- 3 Stone, F. W. and Stratta, J. J. in 'Encyclopedia of Polymer Science and Technology' (Ed. N. M. Bikales), Wiley-Interscience, New York, 1967, Vol. 6, p. 103
- 4 Crump, E. L. in 'Kirk-Othmer Encyclopedia of Chemical Technology', Wiley-Interscience, New York, 1982, Vol. 10, p. 232
- 5 US Pat. 3999358, 1976
- 6 Popescu, R. and Kalmutchi, G. *Rev. Chim.* 1983, **34**, 446 (*Chem. Abstr.* **99**, 111195f)
- 7 Braun, D. B. in 'Handbook of Water-Soluble Gums and Resins' (Ed. R. L. Davidson), McGraw-Hill, New York, 1980, Ch. 19

- 8 Mihailov, M., Nedkov, E. and Goshev, I. *J. Macromol. Sci., Phys. (B)* 1978, **15**, 313
- 9 Allen, R. C. and Mandelkern, L. *J. Polym. Sci., Polym. Phys. Edn.* 1982, **20**, 1465
- 10 Hay, J. N., Sabir, M. and Stevens, R. L. T. *Polymer* 1969, **10**, 187
- 11 Robeson, L. M., Hale, W. F. and Merriam, C. N. *Macromolecules* 1981, **14**, 1644
- 12 Dubrovskii, S. A., Kumpanenko, I. V., Goldberg, V. M. and Kazanskii, K. S. *Vysokomol. Soed.* 1975, **17**, 2733
- 13 Afifi-Effat, A. M. and Hay, J. N. *Eur. Polym. J.* 1972, **8**, 289
- 14 Nakano, A. and Minoura, Y. *J. Appl. Polym. Sci.* 1971, **15**, 927
- 15 Bortel, E., Hodorowicz, S. and Lamot, R. *Makromol. Chem.* 1979, **180**, 2491
- 16 Tatevosyan, E. L., Babich, V. A., Karaseva, N. N. and Tarnorutskii, M. M. *Vysokomol. Soed. (B)* 1974, **16**, 284 (*Chem. Abstr.* **81**, 92083c)
- 17 Goglev, R. S. and Neiman, M. B. *Vysokomol. Soed. (B)* 1967, **9**, 2083 (*Chem. Abstr.* **68**, 13545k)
- 18 Blokhin, V. K., Zarzhetskaya, L. K. and Tsvetova, T. V. *Chem. Abstr.* 1977, **90**, 187811p
- 19 Konishi, K., Sano, Y. and Ajisaka, E., Jap. Pat. 7003225, 1970 (*Chem. Abstr.* **73**, 15786s)
- 20 Vink, H. *Makromol. Chem.* 1963, **67**, 105
- 21 Blyumenfeld, A. B. and Kovarskaya, B. M. *Vysokomol. Soed. (A)* 1970, **12**, 633
- 22 Jain, N. L. and Swinton, F. L. *Eur. Polym. J.* 1967, **3**, 371
- 23 Elias, H. G. *Makromol. Chem.* 1967, **103**, 214
- 24 Cragg, L. H. and van Oeve, H. *Can. J. Chem.* 1961, **39**, 203
- 25 Allen, G., Booth, C., Hurst, S. J., Jones, M. N. and Price, C. *Polymer* 1967, **8**, 391
- 26 Booth, C. and Price, C. *Polymer* 1966, **7**, 85
- 27 Wunderlich, B., 'Macromolecular Physics', Academic Press, New York, 1980, Vol. 3, p. 67
- 28 Watanabe, M., Nagano, S., Sanui, K. and Ogata, N. *Polym. J.* 1986, **18**, 809
- 29 Bu, H. S., Cheng, S. Z. D. and Wunderlich, B. *Polym. Bull.* 1987, **17**, 567
- 30 Guseva, L. N., Mikheyev, Yu. A., Mikheyeva, L. Ye., Sukhareva, S. V. and Toptygin, D. Ya. *Polym. Sci., USSR* 1988, **30**, 1013
- 31 Popov, A. A., Krisyuk, B. E., Blinov, N. N. and Zaikov, G. E. *Eur. Polym. J.* 1981, **17**, 169
- 32 Graff, R. L., Kortleve, G. and Vonk, C. G. *J. Polym. Sci. (B)* 1970, **8**, 735
- 33 Scheirs, J., Bigger, S. W. and Delatycki, O. *J. Mater. Sci.* in press
- 34 Matisova-Rychla, L., Lazar, M. and Rychly, J. *J. Polym. Sci., Polym. Symp.* 1973, **40**, 145
- 35 Rugg, F. M., Smith, J. J. and Bacon, R. C. *J. Polym. Sci.* 1954, **13**, 535
- 36 Mikheev, Yu. A., Guseva, L. N., Mikheeva, L. E., Toptygin, D. Ya. *Vysokomol. Soed. (A)* 1989, **31**, 996 (*Chem. Abstr.* **111**, 134880f)
- 37 Osada, Y. and Sato, M. *J. Polym. Sci., Polym. Lett. Edn.* 1976, **14**, 129
- 38 Winslow, F. H., Aloisio, C. J., Hawkins, W. L., Matreyek, W. and Matsuoka, S. *ACS Div Polym. Chem., Polym. Prepr.* 1963, **4**, 706
- 39 Kovacs, A. J. and Gonthier, A. *Kolloid Z. Z. Polym.* 1972, **250**, 530
- 40 Buckley, C. P. and Kovacs, A. J. *Prog. Colloid Polym. Sci.* 1975, **58**, 44; *Kolloid Z. Z. Polym.* 1976, **254**, 695
- 41 Cheng, S. Z. D. and Wunderlich, B. *J. Polym. Sci., Polym. Phys. Edn.* 1986, **24**, 577
- 42 Short, J. M. and Crystal, R. G. *J. Appl. Polym. Sci. (C) Appl. Polym. Symp.* 1971, **16**, 137
- 43 Mandelkern, L. *J. Appl. Phys.* 1955, **26**, 433
- 44 Keith, H. D. and Padden, F. J. *J. Appl. Phys.* 1964, **35**, 1286
- 45 Scheirs, J., Bigger, S. W. and Delatycki, O. *J. Polym. Sci., Polym. Phys. Edn.* in press
- 46 Fatou, J. G. *Makromol. Chem., Suppl.* 1984, **7**, 131